

Fig. 4. CI chondrite normalized element ratios differ significantly from ratios in Clearwater melt samples (upper part of figure). Element ratios of IVA iron Gibeon agree with ratios in melt samples from Clearwater East. All elements shown in the figures normalized to Gibeon mean taenite and kamacite data (n=17, [15]) (log scale) plot more or less on a horizontal line (lower part of figure). Thus the most likely projectile type based on PGE and Ni would be an iron meteorite. Commas in axis label represent points.

Rochechouart (France): Based on the abundance of Os, Ir, Ni, and Pd in melt samples and subchondritic Os/Ir ratios a IIA magmatic iron asteroid fragment is favoured as projectile type by [16]. [17] report “The projectiles for Rochechouart and Säcksjärvi do not appear to be chondritic in composition but instead stem from fractionated asteroid fragments (Janssens et al., 1977; Palme et al., 1980; Schmidt et al., 1997)”. [17] further report “The PGE patterns of IA and IIIC iron meteorites are identical to the element patterns in the impact melt rocks of Rochechouart and Säcksjärvi”.

Contrary, based on ⁵³Cr excess an ordinary chondrite is favoured by [14]. These authors estimated about 3 wt.% of a chondritic component in the melt.

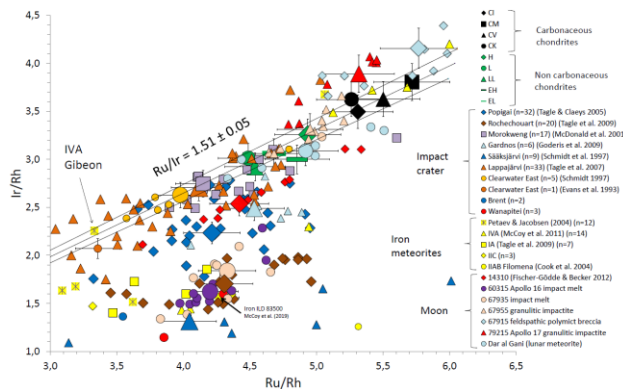


Fig. 5. Ru/Rh versus Ir/Rh mass ratios of Rochechouart [17] and Clearwater East melt samples [7] and meteorite groups [4,8]. Large symbols indicate ratios $\pm 5\%$ (error bars) of summed element masses. Element masses of each subsample, e.g. of the Moon (about 10 ~ 0.04 to 0.1 g subsamples [18]), were summed and the ratios were calculated. Subsample

60315#10 (Apollo 16 impact melt) excluded from calculation. Commas in axis label represent points.

However, Ru/Rh and Ir/Rh from Rochechouart [17] match melt rocks from Apollo 16 landing site [18], IA, IIC, IVA, and ILD 83500 irons [19] (Fig. 5).

Conclusion: The compositional variation in the Ir, Rh and Ru chemistry of chondrites is due to their formation region in the solar nebular. The Ir/Rh mass ratios increases with increasing distance from the sun. Therefore, Ir/Rh and Ru/Rh ratios in melt samples from impact craters allows the differentiation of projectile types. However, diagnostic ratios of Ir, Rh, Ru and Os in impact melts from Clearwater East and Rochechouart impact craters contradict projectile identification by Cr isotopes. Recently, a new indicator for the heliocentric distance of the formation region of chondrites was discovered. [1] report that more reduced materials like enstatite and ordinary chondrites have less negative $\epsilon^{100}\text{Ru}$ compared to more oxidized and volatile-rich materials such as carbonaceous chondrites that formed at greater heliocentric distance. The Ir/Rh mass ratios as an indicator for the heliocentric distance increases with increasing $\epsilon^{100}\text{Ru}$ anomalies. In the future, measurements of Ru isotopes in melt samples (Ru contents of up to 50 ng/g have been determined in Clearwater East melt samples [6,7]) could shed light in controversial projectile identification.

References: [1] Fischer-Gödde M. and Kleine T. (2017) *Nature* 541, 525-527. [2] Fischer-Gödde M. et al. (2011) *Chem Geol* 280, 365 - 383. [3] Palme H. et al. (2014) *Treatise on Geochemistry*, 15–36. [4] Tagle R. and Berlin J. (2008) *Meteoritics & Planet. Sci.*, 43, 541–559. [5] Fischer-Gödde M. et al. (2010) *Geochim. Cosmochim. Acta* 74, 356–379. [6] Evans N. J. et al. (1993) *Geochim. Cosmochim. Acta* 57, 3737–3748. [7] Schmidt G. (1997) *Meteoritics & Planet. Sci.*, 32, 761-767. [8] Petaev M. I. and Jacobsen S. B. (2004) *Meteoritics & Planet. Sci.*, 39, 1685-1697. [9] Fischer-Gödde M. et al. (2015) *Geochim. Cosmochim. Acta* 168, 151-171. [10] Palme H. et al. (1978) *Geochim. Cosmochim. Acta* 42, 313–323. [11] Palme H. et al. (1979) *LPS X*, 2465–2492. [12] Grieve R. A. F. et al. (1981) *Contrib Mineral Petrol* 75, 187-198. [13] McDonald I. (2002) *Meteoritics & Planet. Sci.*, 37, 459-464. [14] Koeberl C. et al. (2007) *Earth Planet Sci Lett* 256, 534–546. [15] McCoy T. J. et al. (2011) *Geochim. Cosmochim. Acta* 75, 6821-6843. App A. Supp data. [16] Janssens M.-J. et al. (1977) *JGR*, 82, 750–758. [17] Tagle R. et al. (2009) *Geochim. Cosmochim. Acta* 73, 4891-4906. [18] Fischer-Gödde M. and Becker H. (2012) *Geochim. Cosmochim. Acta* 77, 135-156. [19] McCoy T.J. et al. (2019) *Geochim. Cosmochim. Acta* 259, 358-370.